

Kinematic Analysis of a Three Degree-of-Freedom Spherical Wrist Actuator

Kok-Meng Lee
Associate Professor

Jianfa Pei
Graduate Research Assistant

Georgia Institute of Technology
The George W. Woodruff School of Mechanical Engineering
Atlanta, GA 30332-0405

ABSTRACT

The paper presents the kinematic analysis of a three degree-of-freedom (DOF) spherical motor which presents some attractive features by combining pitch, roll, and yaw motion in a single joint. Besides being a compact design, the spherical motor possesses no gears or linkages and has no singularities within its workspace. The spherical motor presented in this paper operates on the principle of variable-reluctance (VR). In particular, the theoretical design basic for spherical VR motor was established. The concept feasibility, the design methodology, the motion simulation of a particular design configuration were demonstrated.

1. INTRODUCTION

For applications such as high-speed plasma and laser cutting and coordinate measuring, the orientation must be achieved rapidly and continuously with isotropic resolution in all directions. Several three DOF spherical motor designs have been proposed [1]-[4]. Among these, Lee et al. [5] presented the operational principle of VR stepper motor. Compared with its counterparts, a VR spherical motor has a relatively large range of motion, possesses isotropic properties in motion, and is relatively simple and compact in design. The trade-off, however, is that sophisticated control scheme is required.

The spherical motor referred to in this paper is a ball-joint-like device that consists of two spheres as shown in Fig. 1. These two spheres are concentric and are supported one on the other by bearing rollers in the air gap [6]. The poles on the stator, or the stator poles, are wound by coils and each coil can be energized individually. The ferromagnetic poles are strategically distributed on the stator surface. The rotor poles which have no coil are distributed on the rotor surface. Both the stator poles and the rotor poles are of circular shape. The measurement mechanism of the rotor orientation consists of two circular sliding guides, one sliding block, and three encoders. Lee and Kwan [5]

discussed the VR spherical motor design concept with an aid of a permeance-based analysis. In this paper, the kinematics essential to the operation, design and control of the VR spherical motor are discussed.

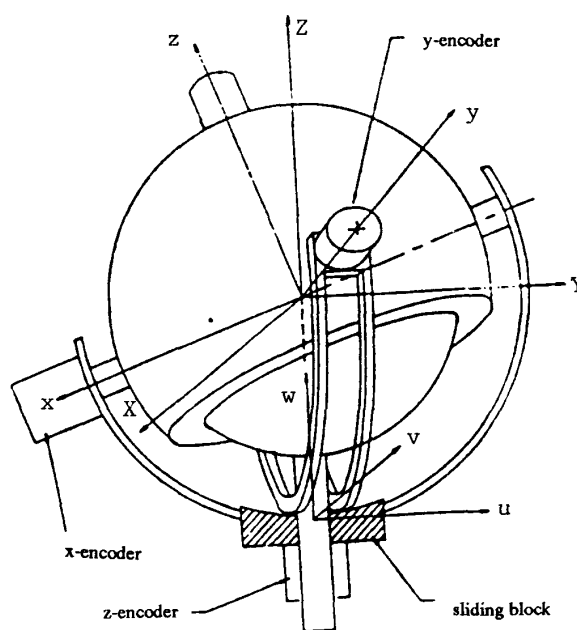


Fig. 1 Basic structure of the VR spherical motor

2. OPERATIONAL PRINCIPLE

The driver of the VR spherical motor is the magnetic attraction force between the rotor and the stator coil excitations. The stator coils can be energized individually using a control circuitry. As the stator coils adjacent to the rotor poles are energized, a magnetic field is generated. The corresponding magnetic flux flows through the air gap between the rotor and the stator. The magnetic attraction is created as the system tries to minimize the energy stored and

reduces the reluctance of the magnetic path. The tangential components of the magnetic force attract the adjacent rotor poles and hence exert a resultant torque on the rotor.

The motor consists of three major components; namely a set of M interconnecting stator poles with electromagnetic coils, a set of N interconnecting rotor poles, and the air gaps formed between pairs of overlapped stator and rotor poles. For the purpose of modeling the kinematics of the spherical motor, both the leakage flux and the fringing flux are neglected and the magnetic system is assumed to be linear. The flux between a stator pole and a rotor pole is thus assumed to flow only through the overlapping area of the two poles. The assumption implies that zero overlapping area corresponds to zero flux. In addition, the flux density distribution in the overlapping area is assumed to be uniform. Thus, the reluctance between the k^{th} stator pole and the l^{th} rotor pole, R_{kl} , is obtained as

$$R_{kl} = \frac{g}{\mu_0 S_{kl}} \quad (1)$$

where μ_0 is the permeability of air, g is the air-gap distance, and S_{kl} is the overlapping area between the k^{th} stator pole and the l^{th} rotor pole. If the rotor pole does not overlap with a stator pole, i.e. $S_{kl} = 0$ or $R_{kl} \rightarrow \infty$, the flux flowing across these two poles is assumed to be zero.

Since the gap reluctances R_{kl} , where $l = 1, 2, \dots, N$, are in parallel, the inverse of the total reluctance T_k is given by the sum of the reciprocal of R_{kl} . The flux flowing through the k^{th} stator coil, λ_k , is thus given by

$$\lambda_k = \left(\frac{1}{T_k} \right) \left[F_k - \frac{\sum_{l=1}^M (F_l / T_l)}{\sum_{l=1}^M (1/T_l)} \right] \quad (2)$$

where F_k is the magneto-motive force (mmf) applied to the k^{th} coil, $k = 1, 2, \dots, M$. The flux flowing through the air-gap between the k^{th} stator pole and the l^{th} rotor pole is denoted by ϕ_{kl} . Since the flux λ_k through a stator coil equals to the sum of the flux of all the air gaps at this coil, ϕ_{kl} , $l = 1, 2, \dots, N$, the flux in each individual air gap is

$$\phi_{kl} = \left(\frac{1}{R_{kl}} \right) \left[F_k - \frac{\sum_{m=1}^M \sum_{n=1}^N (F_m / R_{mn})}{\sum_{m=1}^M \sum_{n=1}^N (1/R_{mn})} \right] \quad (3)$$

Equation (3) represents the flux solution for the spherical motor. The sign of F_k follows the following convention: if the resulting flux density of the coil points outward, then F_k is positive. Otherwise F_k is negative.

From the magnetic circuit solution in Equation (3), the magnetic field energy stored in an air gap is

$$E_{kl} = \frac{1}{2} \phi_{kl}^2 \left(\frac{g}{\mu_0 S_{kl}} \right) \quad (4)$$

Noting that the direction of the torque tends to drive the two poles towards each other in attempt to align the poles, the magnitude of the resulting torque acting on the rotor is derived from the principle of virtual work as

$$t_{kl} = \frac{g}{2\mu_0} \left(\frac{\phi_{kl}}{S_{kl}} \right)^2 \left| \frac{dS_{kl}}{d\theta} \right| \frac{\mathbf{p}_l \times \mathbf{q}_k}{|\mathbf{p}_l \times \mathbf{q}_k|} \quad (5)$$

where $|dS_{kl}/d\theta|$ is the magnitude of the gradient of the overlapping area in spherical coordinates and θ is the angle between the position vectors of the stator and rotor poles.

3. DESIGN CONSIDERATIONS

The geometrical parameters, such as the number of poles and their distribution as well as the size of the poles, directly affect the pole overlappings which in turn affect the motion. The geometrical parameters are designed based on the following considerations.

Range of inclination For simplicity in motion control, it is desired that the poles are evenly spaced on the stator and on the rotor following the pattern of regular polyhedrons. Each vertex of the polyhedron corresponds to the location of one pole. The regular polyhedrons are tetrahedron, octahedron, cube, icosahedron, and dodecahedron. These polyhedrons have four, six, eight, twelve, and twenty vertices, respectively. The choice on the particular pattern influences the range of inclination given by Equation (6).

$$\theta = \Lambda - \frac{\delta}{2} - \psi_2 \quad (6)$$

where θ , Λ , and δ are angles defined in Fig. 2.

Three degree-of-freedom motion The spherical actuator has an infinite number of rotational axes and has three degrees of freedom. With only one rotor pole, a point on the rotor surface can be stabilized in any direction along the tangential inner surface of the stator and thus provide two degrees of freedom motion control. To provide the third

DOF motion which is the spin motion about an axis through the center of the rotor and that of the rotor pole face, a second force must be actuated at an additional rotor pole. Thus, at least two independent torques which are not colinear acting on the rotor are required to generate three DOF orientations. Thus, it is necessary to have more stator poles than rotor poles, or

$$2 \leq N < M. \quad (7)$$

Equation (7) must be valid for the entire range of motion. Furthermore, each of the rotor poles must overlap at least three adjacent stator poles at any instant in order to actuate the rotor pole along any directions on the tangential surface of the stator.

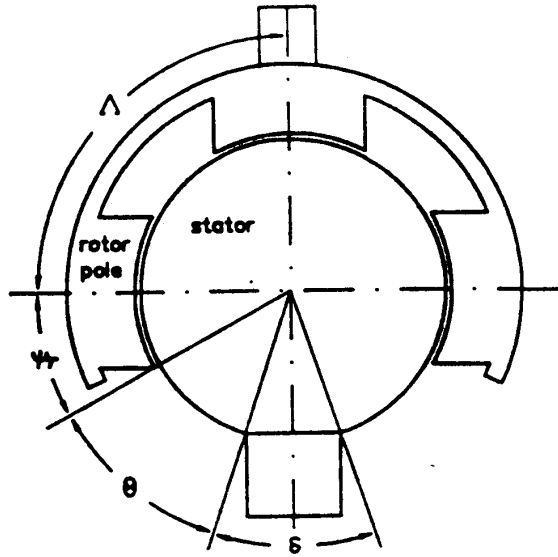


Fig. 2 Illustration of the range of inclination.

Determination of pole size The maximum allowable size of a stator pole is corresponding to the case where two adjacent poles are touching each other.

$$\psi_{1\max} = \frac{1}{2} \cos^{-1} (\mathbf{P}_{si} \cdot \mathbf{P}_{sj}) \quad i \neq j \quad (8)$$

where \mathbf{P}_{si} and \mathbf{P}_{sj} are the position vectors of two adjacent poles. In addition, it is undesirable that any stator pole simultaneously overlaps with more than one rotor pole. The rotor would tend to position itself as the stator pole moves toward the larger overlapping area in an attempt to minimize the reluctance. In order to avoid the stator pole from overlapping with two or more rotor poles, the following inequality is imposed:

$$\psi_1 + \psi_2 < \frac{\Lambda}{2} \quad (9)$$

where Λ is the angle between any two adjacent equally spaced rotor poles.

Avoidance of electro-magnetic singularity The rotor orientation at which the spherical motor loses the ability to generate one or more degrees of freedom is referred here as an electro-mechanical singular point. When all the stator and rotor poles are fully overlapped, $dS_{k\ell} / d\theta = 0$ and no torque would be generated as predicted in Equation (5). Thus, the rotor must not have the same number of evenly spaced poles as that of the stator, i.e. $N \neq M$.

4. KINEMATICS

The kinematics of the spherical motor are represented mathematically using the coordinate frames outlined in the following. A reference coordinate system X-Y-Z is attached to the stator center with its Z-axis along the stator shaft as shown in Fig. 1. Similarly, the body coordinate frame of the rotor, x-y-z, is defined at the rotor center and with its z-axis along the rotor shaft.

An intermediate coordinate frame u-v-w is introduced to describe the coordinate transformation between the X-Y-Z and x-y-z frames. The frame u-v-w is fixed on the sliding block with its u-axis tangent to the x-guide and its w-axis pointing towards the center of the stator along the stator shaft. The v-axis is determined by the orthogonality of the three axes. The w-axis is along the stator shaft and thus coincides with the Z-axis of the frame X-Y-Z. The measurement θ_z is the relative rotation of the frame X-Y-Z with respect to the frame u-v-w.

The parameters used in the derivation of the kinematic equations are illustrated in Fig. 3. It is of interest to derive the forward and inverse kinematics of the spherical motor. Unlike the conventional robotic wrist in which the three joint angles are measured independently, the actuation of the spherical wrist joint requires that the overlapping areas be determined from the three coupled encoder readings, θ_x , θ_y and θ_z .

4.1 Overlapping Area Of Two Poles

The overlapping area between any two adjacent poles determines the resultant tangential force. As indicated by Equation (5), the derivation of the overlapping area is necessary. Consider any two partially overlapping circular poles on a sphere of radius R, where the sizes of the poles are denoted by the half-angles as ψ_1 and ψ_2 as shown in Fig. 4. Two body coordinate frames, X-Y-Z and x-y-z, are attached to the poles ψ_1 and ψ_2 respectively at the origin of the sphere. The orientation of the coordinate frames are

assigned such that the Z-axis and z-axis are pointing along the normal vectors of the poles respectively and that the X-axis and x-axis have a common direction. Thus, the coordinate frame x-y-z can be described with respect to the X-Y-Z frame using the following transformation $[T(\theta)]$ where θ is the angle between the Z-axis and the z-axis.

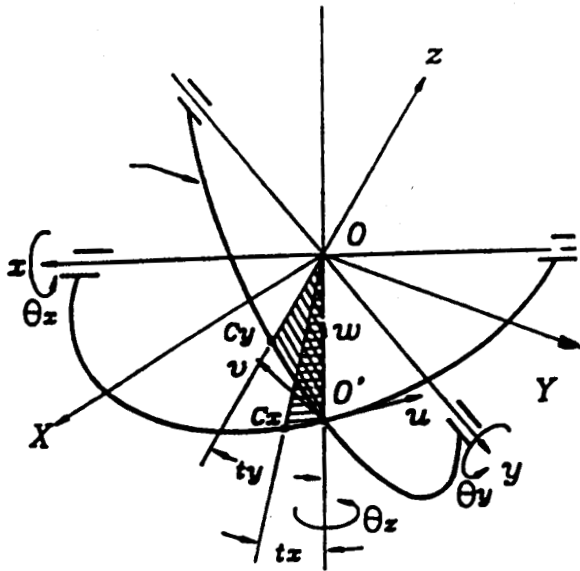


Fig. 3 Parameters used in deriving kinematic equations

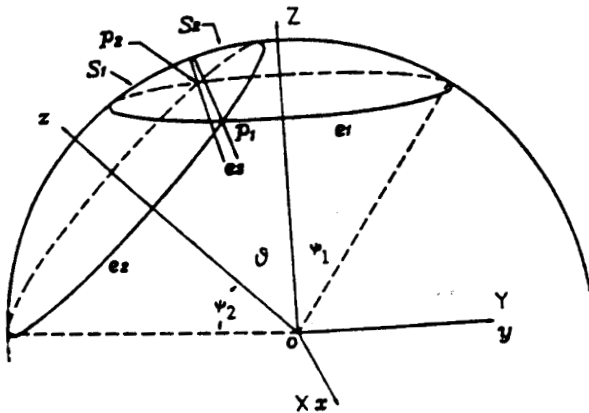


Fig. 4 Geometrical parameters of the two overlapping areas

In parametric form, the circular edge of the pole denoted by the curve e_i , $i = 1$ and 2 , can be written with respect to its own body coordinate frame as

$$\text{curve } e_i: \begin{cases} x^2 + y^2 = (R s_{\psi_i})^2 \\ z = R c_{\psi_i} \end{cases} \quad (10)$$

where the notations c_{ψ_i} and s_{ψ_i} refer to the trigonometric cosine and sine functions of the angle ψ_i respectively.

In the following derivation, the coordinates are written with respect to the X-Y-Z frame. Using the transformation matrix $[T(\theta)]$ the curve e_2 can be described by

$$\begin{cases} x^2 + (y + R c_{\psi_1} s_{\theta})^2 / c_{\theta}^2 = (R s_{\psi_2})^2 \\ x^2 + (z + R c_{\psi_1} c_{\theta})^2 / s_{\theta}^2 = (R s_{\psi_2})^2 \end{cases} \quad (11)$$

The position vectors of the two intersecting points are P_1 and P_2 which are symmetrical about the YZ plane and can be derived by solving Equations (10) and (11) simultaneously. Thus, the position vector P_1 is obtained as

$$P_1 = \begin{bmatrix} \frac{R}{s_{\theta}} \sqrt{[(s_{\psi_1} s_{\theta})^2 - (c_{\psi_1} c_{\theta} - c_{\psi_2})^2]} \\ -\frac{R}{s_{\theta}} (c_{\psi_1} c_{\theta} - c_{\psi_2}) \\ R c_{\psi_1} \end{bmatrix} \quad (12)$$

and point p_2 is a mirror image of point p_1 . If a plane is defined to pass through p_1 and p_2 and the origin of the sphere, the plane would divide the overlapping area S into two parts, S_1 and S_2 . Let the intersecting contour be denoted by the curve e_3 and the angle between plane op_1p_2 and the XZ plane be ρ . The intersecting contour e_3 is derived with respect to X-Y-Z frame as

$$\begin{cases} x^2 + y^2 / s_{\rho}^2 = R^2 \\ x^2 + z^2 / c_{\rho}^2 = R^2 \end{cases} \quad (13)$$

where

$$\rho = \tan^{-1} \left(\frac{c_{\psi_2} - c_{\psi_1} c_{\theta}}{c_{\psi_1} s_{\theta}} \right) \quad (14)$$

From the projection of the curves e_i , $i = 1, 2$, and 3 on the XY plane given in Equations (10), (11) and (13), the overlapping area is computed from the following integral:

$$A_i = \iint_D \frac{R \, dx \, dy}{\sqrt{R_i^2 - x^2 - y^2}} \quad i = 1, 2 \quad (15)$$

where A_i and D_i are the areas bounded by e_i and e_3 on the spherical surface and the corresponding projections on XY plane respectively. By carrying out the integration, the overlapping area is found to be

$$A = \sum_{i=1}^2 A_i \quad (16)$$

where

$$A_i = R^2 \left\{ [1 + \text{Sgn}(c_{\psi_i} c_{\theta} - c_{\psi_{(i+1)}})] (1 - c_{\psi_i}) \pi + \right.$$

$$\left. 2 \text{Sgn}(c_{\psi_i} c_{\theta} - c_{\psi_{(i+1)}}) [\Delta_i c_{\psi_i} - \sin^{-1}(c_{\Gamma_i} s_{\Delta_i})] \right\} \quad \text{where} \quad (17)$$

$$\Gamma_i = \tan^{-1} \left(\frac{c_{\psi_{(i+1)}} - c_{\psi_i} c_{\theta}}{c_{\psi_i} s_{\theta}} \right) \quad (18)$$

and

$$\Delta_i = \tan^{-1} \left(\frac{\sqrt{(s_{\psi_i} s_{\theta})^2 - [c_{\psi_i} c_{\theta} - c_{\psi_{(i+1)}}]^2}}{|c_{\psi_i} c_{\theta} - c_{\psi_{(i+1)}}|} \right) \quad (19)$$

where $\psi_3 = \psi_1$ and the function $\text{sgn}(x)$ is 1 if x is positive or -1 if x is negative.

4.2 Forward Kinematics

The forward kinematics is to determine the rotor orientation given the readings of the three encoders. The initial or zero readings of θ_x and θ_y are defined when c_x and c_y coincides, which are the middle points of the x- and y-guides. The guides intersect at point O' , which is the origin of frame u-v-w, and is measured by the sliding angles t_x and t_y along the x-, and y-guide from c_x and c_y respectively as shown in Fig. 3. t_x and t_y are

$$t_x = \tan^{-1} (\tan \theta_y \cos \theta_z) \quad (20)$$

$$t_y = \tan^{-1} (\tan \theta_x \cos \theta_z) \quad (21)$$

The unit vectors along the u-, v- and w-axis, with respect to the xyz frame is determined by noting the followings: The vector u is given by the derivative of $\underline{O'}$ with respect to t_x ; the unit vector v is defined by the cross-product of w and u ; and the unit vector w is in the opposition direction of $\underline{O'}$. Since both the w-axis of the frame u-v-w and the Z-axis of the frame X-Y-Z are defined along the stator shaft, θ_z is the relative rotation of frame X-Y-Z about the w-axis of frame u-v-w. The forward kinematic transformation is thus given by

$${}^{XYZ}_T = \begin{bmatrix} n_x & o_x & a_x \\ n_y & o_y & a_y \\ n_z & o_z & a_z \end{bmatrix} \quad (22)$$

$$n_x = c_{tx} c_{\theta z} \quad (23a)$$

$$n_y = -c_{tx} s_{\theta z} \quad (23b)$$

$$n_z = -s_{tx} \quad (23c)$$

$$o_x = -s_{tx} s_{\theta x} c_{\theta z} + c_{\theta x} s_{\theta z} \quad (23d)$$

$$o_y = s_{tx} s_{\theta x} s_{\theta z} + c_{\theta x} c_{\theta z} \quad (23e)$$

$$o_z = -c_{tx} s_{\theta x} \quad (23f)$$

$$a_x = s_{tx} c_{\theta x} c_{\theta z} + s_{\theta x} s_{\theta z} \quad (23g)$$

$$a_y = -s_{tx} c_{\theta x} s_{\theta z} + s_{\theta x} c_{\theta z} \quad (23h)$$

$$a_z = c_{tx} c_{\theta x} \quad (23i)$$

Hence, for a given set of encoder readings, the rotor orientation can be determined from Equations (22) and (23a-i). The overlapping areas of each air-gap can be found from Equations (16) to (19).

4.3 Inverse Kinematics

The inverse kinematics involve solving Equations (22) and (23) for the encoder measurements θ_x , θ_y , and θ_z required for a specified rotor orientation.

The rotor orientation defined by ${}^{XYZ}T_{xyz}$ is determined from Equations (23f) and (23i), where yields

$$\theta_x = \text{atan2}(-o_z, a_z) \quad (24)$$

Similarly, θ_z is solved from Equations (23a) and (23b) resulting in

$$\theta_z = \text{atan2}(-n_y, n_x) \quad (25)$$

θ_y is related to Equations (23a)-(23i) implicitly via t_x . Using the following relationship

$${}^{XYZ}T_{xyz} {}^{xyz}T_{uvw} = {}^{XYZ}T_{uvw} \quad (26)$$

the element at the first row and the third column of the resulting equation is given as

$$-n_x^s t_x - o_x^c t_x^s \theta_x + a_x^c t_x^c \theta_x = 0 \quad (27)$$

or

$$\tan t_x = \frac{a_x^c \theta_x - o_x^s \theta_x}{n_x} \quad (28)$$

The measurement θ_y can be solved by substituting $(\tan t_x)$ and θ_x from Equations (20) and (24) into Equation (28) respectively, or

$$\theta_y = \text{atan2}(-a_x a_z - o_x o_z, n_x a_z) \quad (30)$$

In terms of roll-yaw-pitch angles, α , β and γ , the inverse kinematics equations are obtained as

$$\theta_x = \text{atan2}(-c_\beta s_\gamma, -s_\beta) \quad (31a)$$

$$\theta_y = \text{atan2}(-c_\alpha s_\beta c_\beta, c_\alpha c_\beta^2 c_\gamma) \quad (31b)$$

$$\theta_z = \text{atan2}(-s_\alpha c_\beta, c_\alpha c_\beta) \quad (31c)$$

5. CONCLUSIONS

This paper presented the kinematic analysis of a three degree of freedom spherical wrist actuator. The actuation of the ball-joint-like spherical wrist has been described in terms of overlapping areas between the stator and rotor poles. An exact relationship of the overlapping area in three dimensional space have been derived. It is expected that the inverse and forward kinematics presented in this paper provide significant physical insights to the basis of design,

modeling, and simulation in future research of spherical motors.

Acknowledgements This work is supported by the National Science Foundation under grant number DMC 8810146.

Bibliography

- [1] Vachtsevanos, G.J., Davey, K., and Lee, K.M., "Development of a Novel Intelligent Robotic Manipulator", IEEE Control Systems Magazine, June 1987.
- [2] Hollis, R.L., Allan, A.P. and Salcudean, S., "A Six Degree-of-freedom Magnetically Levitated Variable Compliance Fine Motion Wrist", Fourth Int'l Symp. on Robotics Research, Santa Cruz, August, 1987.
- [3] Kaneko, K., Yamada, I. and Itao, K. "A Spherical DC Servo Motor with Three Degrees of Freedom", ASME, Dyn. Systems & Control Div., Vol. 11, 1988, p. 433.
- [4] Lee, K.M., Vachtsevanos, G., and Kwan, C.K., "Development of a Spherical Stepper Wrist Motor", IEEE Int. Conf. on Robotics & Automation, 1988. Also in J. Intell. and Robot. Systems, 1, 1988, p.225.
- [5] Lee, K.M. and Kwan, C., "Design Concept Development of a Spherical Stepper for Robotic Applications", IEEE Journal of Robotics and Automation, Vol. 7 No. 1, Feb. 1991.